

Alkali Metals and the Color of Brown Dwarfs

Adam Burrows¹

¹ Department of Astronomy and Steward Observatory,
The University of Arizona, Tucson, AZ 85721, USA

Abstract. I summarize some of the consequences for the optical and very-near-infrared spectra of T dwarfs (in particular) and brown dwarfs (in general) of their possible dominance by the neutral alkali metal lines. As a byproduct of this study, I estimate the true optical color of “brown” dwarfs.

1 Introduction

The early discovery phase for L dwarfs and T dwarfs has ended and a major focus is now on their characterization. The atmospheres of brown dwarfs are dominated by H₂, H₂O, CH₄, NH₃, the neutral alkali metals, and grains, but how theory translates this basic knowledge into effective temperatures, gravities, and compositions has yet to be determined. Establishing the spectral and color diagnostics that are most appropriate for L/T studies is complicated by ambiguities in the cloud/grain models and a paucity of opacity data. In particular, though T dwarfs are being informally defined by their methane features at 1.7 μm and 2.2 μm , the methane database itself is far from complete. The methane opacities on the red side of the *H* band are certainly in error by a factor of 3 to 5 (witness Gliese 229B[1]) and the hot bands are completely missing. The latter means that even the sign of the opacity’s dependence upon temperature can be in error. Nevertheless, there has been great overall progress towards understanding what makes these objects unique and what their spectra are telling us. In this paper, I sidestep a comprehensive study of these issues and summarize three interesting topics in brown dwarf theory that have emerged of late. They are 1) what determines T dwarf spectra shortward of 1.0 micron, 2) what is the true color of a “brown” dwarf, and 3) what is the effect of heavy element depletion (“rainout”) on the abundance profiles of the neutral alkali metal atoms. A subtext of this contribution is the central importance of the alkali metals in spectrum formation.

2 The Short-Wavelength Spectra of T Dwarfs

Employing the scheme of Burrows, Marley, and Sharp[2] (hereafter BMS), we can derive the neutral alkali opacities as a function of wavelength. Figure 1 depicts the abundance-weighted opacities of the dominant neutral alkali metal lines at 1500 K and 1 bar. This opacity spectrum has a bearing on the suggestion by BMS that the strong continuum absorption seen in all T dwarf spectra in

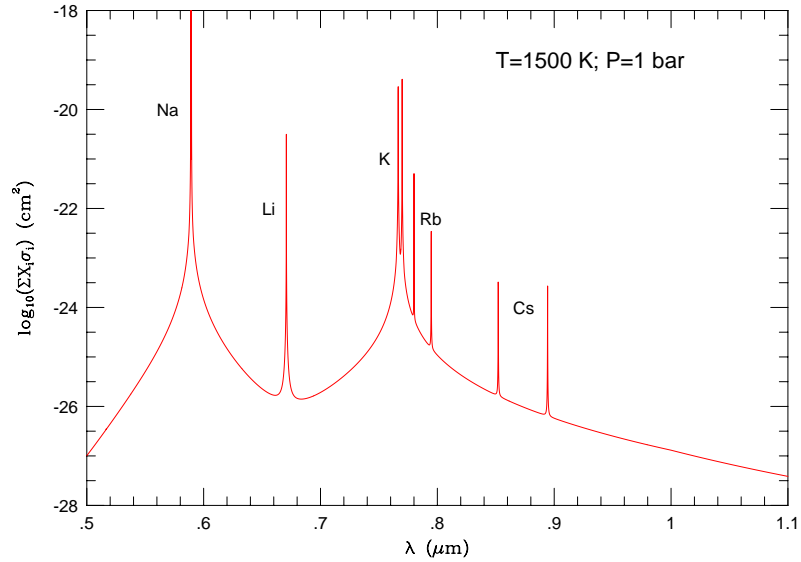


Fig. 1. Plotted is the abundance-weighted cross section spectrum for the neutral alkali metals Na, K, Cs, Rb, and Li at 1500 K and 1 bar pressure, using the theory of BMS. The most important spectral lines for each species are clearly marked.

the near-infrared from $0.8 \mu\text{m}$ to $1.0 \mu\text{m}$, previously interpreted as due to an anomalous population of red grains[3] or in part due to high-altitude silicate clouds[4], is most probably due to the strong red wings of the K I doublet at $\sim 7700 \text{ \AA}$. This is demonstrated in Figure 2, in which several possible theoretical spectra are compared with the observed spectrum for Gliese 229B in the near-infrared[2]. Tsuji et al. [5] also identified the K I doublet as one of the agents of absorption shortward of one micron, but they needed silicate grains as well to reproduce the Gliese 229B observations. BMS conclude that the K I resonance doublet alone is responsible, though, given the remaining ambiguity in its line shape, one can't completely eliminate the presence of grains as secondary agents.

As Figure 2 suggests, the BMS theory also explains the WFPC2 *I* band ($M_I \sim 20.76$; theory = 21.0) and *R* band ($M_R \sim 24.0$; theory = 23.6) measurements made of Gl 229B[6], with the Na D lines at 5890 \AA helping to determine the strength of the *R* band. BMS predicted not only that there would be a large trough in a T dwarf spectrum at 7700 \AA due to the K I resonance, but that

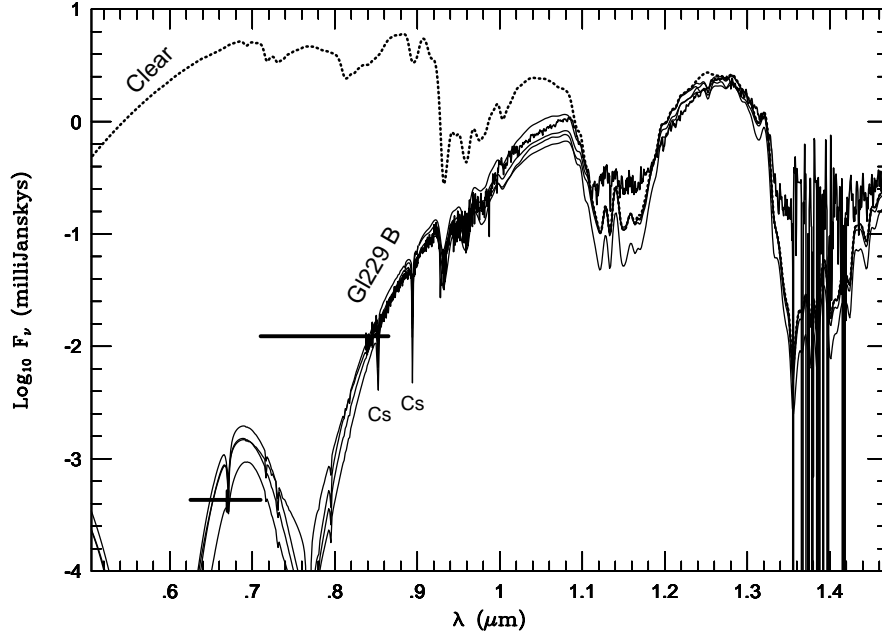


Fig. 2. The log of the absolute flux (F_ν) in milliJanskys versus wavelength (λ) in microns from $0.5 \mu\text{m}$ to $1.45 \mu\text{m}$ for Gliese 229 B, according to Leggett et al. [1] (heavy solid), and for four theoretical models (light solid) described in BMS. Also included is a model, denoted “Clear” (dotted), without alkali metals and without any ad hoc absorber due to grains or haze. The horizontal bars near $0.7 \mu\text{m}$ and $0.8 \mu\text{m}$ denote the WFCPC2 *R* and *I* band measurements of Golimowski et al. [6]. Figure taken from BMS.

the spectrum of a T dwarf would peak between the Na D and K I absorption troughs at 5890 \AA and 7700 \AA , respectively. This prediction was recently verified by Liebert et al. [7] for the T dwarf SDSS 1624+00.

Furthermore, the $1.17 \mu\text{m}$ and $1.24 \mu\text{m}$ subordinate lines of excited K I have been identified in T dwarfs [8,9,10]. Since these subordinate lines are on the crown of the *J* band, they allow one to probe the deeper layers at higher temperatures. Figure 3 portrays for a representative G1 229B model the dependence on wavelength of the “brightness” temperature, here defined as the temperature at which the photon optical depth is $2/3$. Such plots clearly reveal the temperature layers probed with spectra and provide a means to qualitatively gauge composition profiles. Specifically, for the G1 229B model, the detection of the subordinate lines of potassium indicates that we are there probing to $\sim 1600 \text{ K}$, while the detection of the fundamental methane band at $3.3 \mu\text{m}$ (not shown in Figure 3) means that we are probing to only $\sim 600 \text{ K}$.

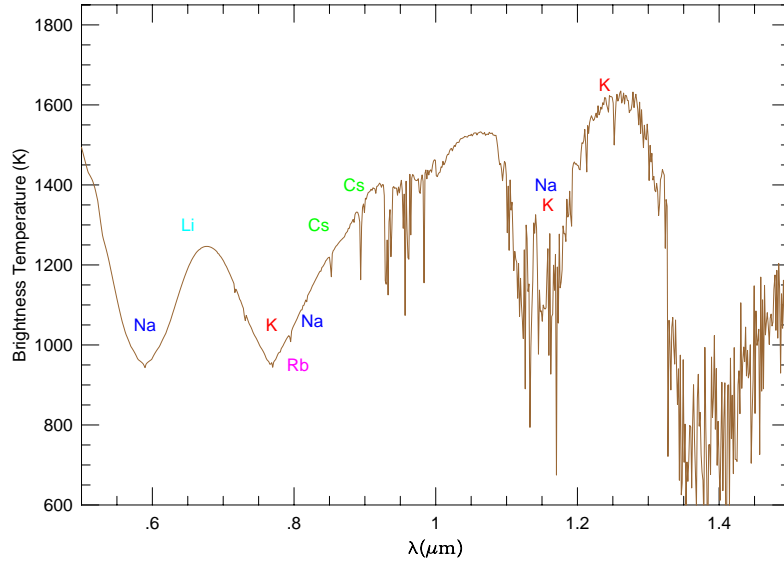


Fig. 3. The brightness temperature in Kelvin versus wavelength in microns from 0.5 μm to 1.5 μm of a simple model of Gliese 229B. The brightness temperature for a given wavelength is defined as the temperature of the layer at which $\tau_\lambda = 2/3$. The identity of the alkali metal atom responsible for a given feature is indicated. See text for discussion.

3 The Color of Brown Dwarfs

Figure 1 shows that the Na D doublet should dominate the optical portion of the spectrum. Since it suppresses the green wavelengths and “brown” is two parts red, one part green, and very little blue, brown dwarfs should not be brown. In fact, our recent calculations suggest that they are red to purple, depending upon the exact shape of the line wings of Na D, the abundance of the alkalis, the presence of high-altitude clouds, and the role of water clouds at lower T_{eff} s ($\lesssim 500$ K). A mixture of red and the complementary color to the yellow of the Na D line makes physical sense. It is the *complementary* color, not the *color*, of the Na D line(s) because Na D is seen in absorption, not emission. Indeed, the recent measurement of the spectrum of the L5 dwarf 2MASSW J1507 from 0.4 μm to 1.0 μm (I.N. Reid and J.D. Kirkpatrick, in preparation) indicates that this L dwarf is magenta in (optical) color. This is easily shown with a program

that generates the RGB equivalent of a given optical spectrum (in this instance, R:G:B::1.0:0.3:0.42, depending upon the video “gamma”). Hence, after a quarter century of speculation and ignorance, we now have a handle on the true color of a brown dwarf — and it is not brown.

4 Rainout and the Alkali Metals

As shown by Burrows and Sharp[11], Fegley and Lodders[12], and Lodders[13], the alkali metals are less refractory than Ti, V, Ca, Si, Al, Fe, and Mg and survive in abundance as neutral atoms in substellar atmospheres to temperatures of 1000 K to 1500 K. This is below the 1600 K to 2500 K temperature range in which the silicates, iron, the titanates, corundum, and spinel, etc. condense and rainout. The rainout of refractory elements such as silicon and aluminum ensures that Na and K are not sequestered in the feldspars high albite ($\text{NaAlSi}_3\text{O}_8$) and sanadine (KAlSi_3O_8) at temperatures at and below 1400 K, but are in their elemental form down to ~ 1000 K. Hence, in the depleted atmospheres of the cool T dwarfs and late L dwarfs, alkali metals quite naturally come into their own. Figures 4 and 5 demonstrate the role of rainout by depicting the profiles of the relative abundances of the main reservoirs of the alkali metals, with and without rainout as crudely defined in reference [11]. As is clear from a comparison of these two figures, rainout and depletion of heavy metals can result in a significant enhancement in the abundances at altitude (lower temperatures) of the neutral alkali metal atoms, in particular sodium and potassium.

Figure 2 demonstrates the naturalness with which the potassium resonance lines alone fit the observed near-infrared/optical spectrum of Gl 229B. Curiously, in the metal-depleted atmospheres of T dwarfs the reach of the K I doublet is one of the broadest in astrophysics, its far wings easily extending more than 1500 Å to the red and blue. With rainout, below ~ 1000 K both sodium and potassium exist as sulfides (Na_2S and K_2S)[13]. Without rainout, complete chemical equilibrium at low temperatures requires that sodium and potassium reside in the feldspars. If such compounds formed and persisted at altitude, then the nascent alkali metals would be less visible, particularly in T dwarfs. By modeling spectra with and without the rainout of the refractories and comparing to the emerging library of T dwarf spectra[10,14,15,16], the degree of rainout and the alkali composition profiles in brown dwarf atmospheres can be approximately ascertained.

5 Conclusion

L and T dwarf spectra are unique among “stars” and require new databases, approaches, and thinking to fully understand. Exploring as we are new worlds, we will require new tools and instincts with which to navigate. Along with accurate cloud models, methane, and water, the alkali metals hold the key to unraveling the mysteries of the substellar objects that we now know inhabit the solar neighborhood in abundance.

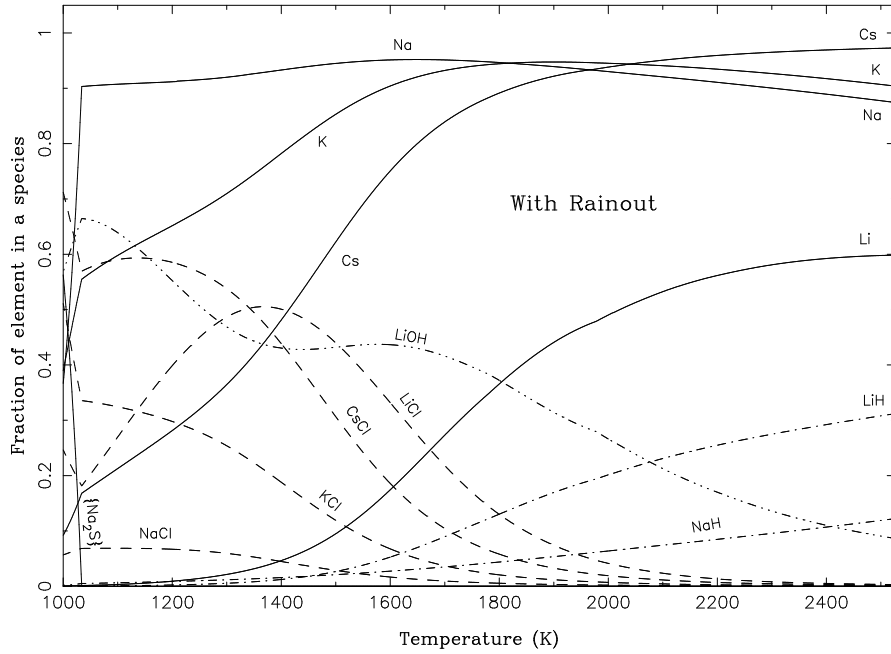


Fig. 4. The fractional abundances of different chemical species involving the alkali elements Li, Na, K and Cs for a Gliese 229B model, with rainout as described in Burrows and Sharp[11]. The temperature/pressure profile for a $T_{\text{eff}} = 950$ K and $g = 10^5$ cm s^{-2} model, taken from Burrows et al. [17], was used. Each curve shows the fraction of the alkali element in the indicated form out of all species containing that element. All species are in the gas phase except for the condensates, which are in braces { and }. The solid curves indicate the monatomic gaseous species Li, Na, K and Cs, the dashed curves indicate the chlorides, the dot-dashed curves indicate the hydrides and the triple dot-dashed curve indicates LiOH. Due to rainout, at lower temperatures there is a dramatic difference with the no-rainout, complete equilibrium calculation (Figure 5); high albite and sanidine do not appear, but instead at a much lower temperature the condensate Na_2S (disodium monosulfide) forms, as indicated by the solid line in the lower left of the figure. The potassium equivalent, K_2S , also forms, but it does so below 1000 K and is not indicated here. The difference between this Figure and Figure 5 is that almost all the silicon and aluminum have been rained out at higher temperatures, so that no high albite and sanidine form at lower temperatures. Figure taken from BMS.

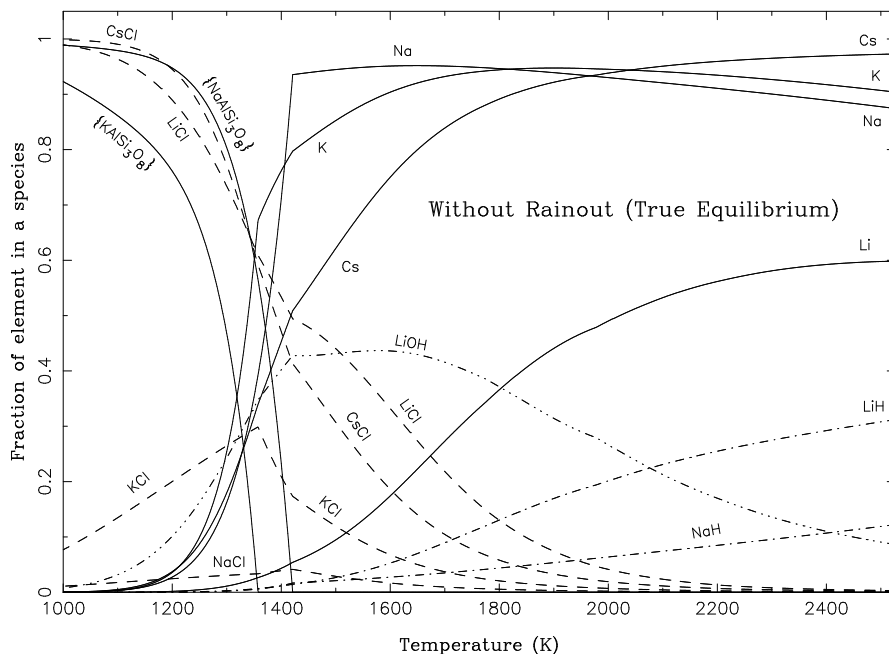


Fig. 5. The fractional abundances of different chemical species involving the alkali elements Li, Na, K and Cs for a Gliese 229B model, assuming complete (true) chemical equilibrium and no rainout (disfavored). The temperature/pressure profile for a $T_{\text{eff}}=950$ K and $g = 10^5 \text{ cm s}^{-2}$ model, taken from Burrows et al. [17], was used. Each curve shows the fraction of the alkali element in the indicated form out of all species containing that element, *e.g.*, in the case of sodium, the curves labeled as Na, NaCl, NaH and NaAlSi₃O₈ are the fractions of that element in the form of the monatomic gas and three of its compounds. All species are in the gas phase except for the condensates, which are in braces { and }. The solid curves indicate the monatomic gaseous species Li, Na, K and Cs and the two condensates NaAlSi₃O₈ and KAlSi₃O₈, *i.e.*, high albite and sanidine, respectively, the dashed curves indicate the chlorides, the dot-dashed curves indicate the hydrides and the triple dot-dashed curve indicates LiOH. Figure taken from BMS.

Acknowledgments:

I thank my long-time collaborators, Jonathan Lunine, Bill Hubbard, and Mark Marley, for simulating input and both Davy Kirkpatrick and Neill Reid for an advanced glimpse at their stunning 2MASSW J1507 spectrum. This work was supported in part by NASA under grants NAG5-7073 and NAG5-7499.

References

1. S. Leggett, D.W. Toomey, T. Geballe, R.H. Brown: *Astrophys. J.* **517**, L139 (1999)
2. A. Burrows, M.S. Marley, C.M. Sharp: *Astrophys. J.* **531**, 438 (2000).

3. C.A. Griffith, R.V. Yelle, M.S. Marley: *Science* **282**, 2063 (1998)
4. F. Allard, P.H. Hauschildt, D.R. Alexander, S. Starrfield: *Annu. Rev. Astron. Astrophys.* **35**, 137 (1997)
5. T. Tsuji, K. Ohnaka, W. Aoki: *Astrophys. J.* **520**, L119 (1999)
6. D.A. Golimowski, et al. : *Astron. J.* **115**, 2579 (1998)
7. J. Liebert, I.N. Reid, A. Burrows, A.J. Burgasser, J.D. Kirkpatrick, J.E. Gizis: *Astrophys. J.* **533**, 155 (2000)
8. M.A. Strauss, et al. : *Astrophys. J.* **522**, L61 (1999)
9. Z.I. Tsvetanov, et al. : *Astrophys. J.* **531**, L61 (2000)
10. I.S. McLean, et al. : *Astrophys. J.* **533**, L45 (2000)
11. A. Burrows, C.M. Sharp: *Astrophys. J.* **512**, 843 (1999)
12. B. Fegley, K. Lodders: *Astrophys. J.* **472**, L37 (1996)
13. K. Lodders: *Astrophys. J.* **519**, 793 (1999)
14. A. Burgasser, et al. : *Astrophys. J.* **522**, L65 (1999)
15. A. Burgasser, et al. : *Astrophys. J.* **531**, L57 (2000)
16. S. Leggett, *et al.*: *Astrophys. J.* **536**, L35 (2000)
17. A. Burrows, M. Marley, W.B. Hubbard, J.I. Lunine, T. Guillot, D. Saumon, R. Freedman, D. Sudarsky, C. Sharp: *Astrophys. J.* **491**, 856 (1997)